

Terahertz backscattering behavior of various absorbing materials

C. Wu^a, A. J. Gatesman^a, L. DeRoeck^a, T. Horgan^a, R. H. Giles^a, and W. E. Nixon^b

^aSubmillimeter-Wave Technology Laboratory, University of Massachusetts Lowell
Lowell, MA 01854

^bU.S. Army National Ground Intelligence Center
Charlottesville, VA 22911

ABSTRACT

The Submillimeter-Wave Technology Laboratory (STL) at the University of Massachusetts Lowell has investigated the electromagnetic scattering behavior of various broadband absorbers. Several absorbing materials were tested in a compact radar range operating at a center frequency of 160 GHz. The polarimetric radar cross section was measured at elevation angles from 15° to 75°. In addition to the backscattering behavior, the normal incidence transmittance of the materials was evaluated.

Keywords: Terahertz, THz, absorbers, scattering, radar

1. INTRODUCTION

Absorbing materials are commonly utilized in a wide variety of optical systems such as antenna test ranges and imaging systems [1]. High performance absorbing materials are particularly important in compact radar range design. A number of studies measuring the reflective behavior of absorbing materials at terahertz (THz) frequencies have been performed [2], [3]. However, the backscattering behavior of absorbers is not well understood. The purpose of this research was to investigate the backscattering behavior of several absorbing materials in a compact radar range at terahertz frequencies.

Several different types of structures were characterized including wedged, pyramidal, and bulk absorbers. The 160 GHz radar cross section (RCS) of the materials was characterized over a range of azimuth and elevation angles. Due to experimental limitations, the measurements presented here were performed over a limited range of angles and over a narrow range of frequencies centered at 160 GHz. It is understood that many of the materials have optimal scattering characteristics at other frequencies and angles of incidence. For example, many of the materials were not designed for use at the look angles covered in this study. Furthermore, two of the absorbers were specifically designed for microwave applications. Therefore, the intent of this study was not necessarily to provide an evaluation of which absorber had best performance, but rather to better understand the general backscattering behavior of dielectric structures at terahertz frequencies.

2. MATERIAL DESCRIPTION

Seven absorbing materials were selected for characterization and are shown in Figure 1. The materials were FIRAMTM-160, FIRAMTM-500-red, and FIRAMTM-500-black (Submillimeter-Wave Technology Laboratory) [4], Rex radar-absorbing Mat (Marktek Inc.), AEL absorbing material (Advanced ElectroMagnetics Inc.), neoprene wetsuit (Rubatex International, LLC), and Spaced-qualified Tessalating Terahertz RAM (Thomas Keating Ltd.). Each absorber was approximately 24 in. x 24 in. in size. TK THz RAM was provided in 4 in. x 4 in. tiles, therefore, a 24 in. x 24 in. area was assembled from 36 individual tiles.

Report Documentation Page				Form Approved OMB No. 0704-0188	
Public reporting burden for the collection of information is estimated to average 1 hour per response, including the time for reviewing instructions, searching existing data sources, gathering and maintaining the data needed, and completing and reviewing the collection of information. Send comments regarding this burden estimate or any other aspect of this collection of information, including suggestions for reducing this burden, to Washington Headquarters Services, Directorate for Information Operations and Reports, 1215 Jefferson Davis Highway, Suite 1204, Arlington VA 22202-4302. Respondents should be aware that notwithstanding any other provision of law, no person shall be subject to a penalty for failing to comply with a collection of information if it does not display a currently valid OMB control number.					
1. REPORT DATE 2009		2. REPORT TYPE		3. DATES COVERED 00-00-2009 to 00-00-2009	
4. TITLE AND SUBTITLE Terahertz backscattering behavior of various absorbing materials				5a. CONTRACT NUMBER	
				5b. GRANT NUMBER	
				5c. PROGRAM ELEMENT NUMBER	
6. AUTHOR(S)				5d. PROJECT NUMBER	
				5e. TASK NUMBER	
				5f. WORK UNIT NUMBER	
7. PERFORMING ORGANIZATION NAME(S) AND ADDRESS(ES) U.S. Army National Ground Intelligence Center, Charlottesville, VA, 22911				8. PERFORMING ORGANIZATION REPORT NUMBER	
9. SPONSORING/MONITORING AGENCY NAME(S) AND ADDRESS(ES)				10. SPONSOR/MONITOR'S ACRONYM(S)	
				11. SPONSOR/MONITOR'S REPORT NUMBER(S)	
12. DISTRIBUTION/AVAILABILITY STATEMENT Approved for public release; distribution unlimited					
13. SUPPLEMENTARY NOTES in Terahertz Physics, Devices, and Systems III: Advanced Applications in Industry and Defense, edited by Mehdi Anwar; Nibir K. Dhar; Thomas W. Crowe, Proceedings of SPIE Vol. 7311 (SPIE, Bellingham, WA 2009) 73110M. U.S. Government or Federal Rights License					
14. ABSTRACT see report					
15. SUBJECT TERMS					
16. SECURITY CLASSIFICATION OF:			17. LIMITATION OF ABSTRACT Same as Report (SAR)	18. NUMBER OF PAGES 12	19a. NAME OF RESPONSIBLE PERSON
a. REPORT unclassified	b. ABSTRACT unclassified	c. THIS PAGE unclassified			

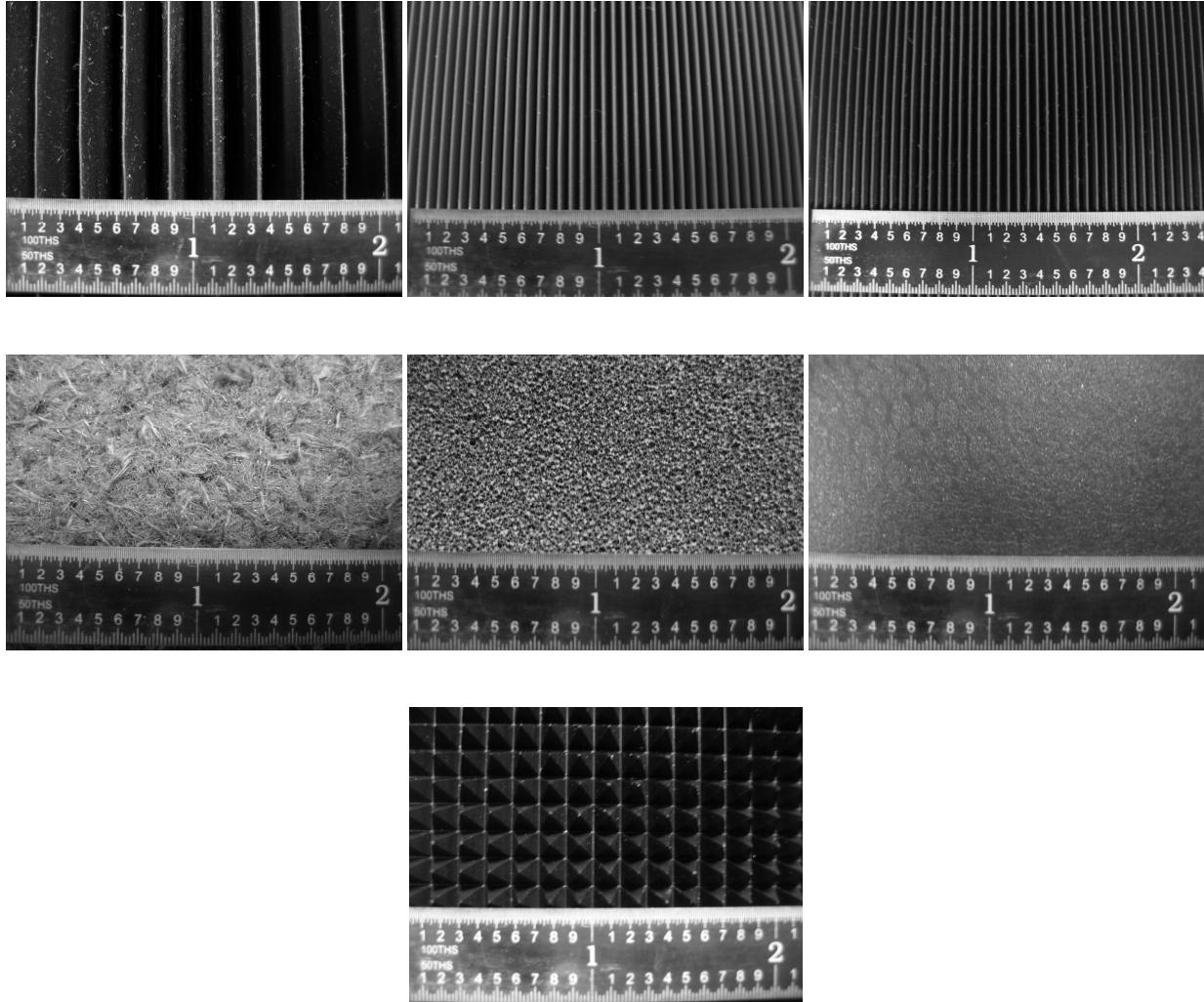


Fig. 1. FIRAM™-160, FIRAM™-500-red, FIRAM™-500-black, Rex Mat, AEL, neoprene wetsuit and TK THz RAM are shown from left to right.

3. MEASUREMENT SYSTEM DESCRIPTION

The 160 GHz compact range, shown in Figure 2, consisted of a transceiver, a main collimating antenna, a target/calibration positioning system, and a data-acquisition system. Specific details of the 160 GHz compact radar range can be found in prior publications [5], [6]. The target positioning system automated the target positioning in both azimuth and elevation. The low-RCS pylon consisted of a 4 feet long aluminum support with an ogive cross-section. The pylon was tilted forward a minimum of 10° from the vertical to reduce backscattering. Figure 3 shows the FIRAM™-500-red placed on the pylon. The compact range walls and ceiling were covered with FIRAM™-160 which were mounted onto large movable panels and allowed the orientation of the anechoic to be optimized to reduce backscattering and minimize target-chamber interactions.

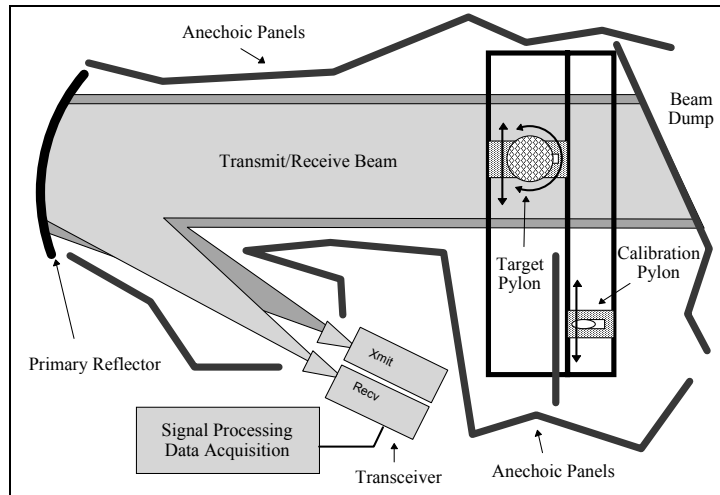


Fig. 2. Schematic of STL's 160 GHz compact range.



Fig. 3. Sample of FIRAM™-500-red placed on the low-RCS target pylon. The smaller pylon in front of the target pylon supported an in-scene phase calibration object.

4. MEASUREMENT RESULTS

4.1 Radar cross section of the absorbing materials

The radar cross section of the absorbing materials was measured at elevation angles from 15° to 75° in 10° increments, and is shown in Figures 4-10. For each elevation angle, the materials were rotated in azimuth from 0° to 360° , in 0.05° increments. For the wedged absorbers, the azimuth angle was defined such that at 90° and 270° azimuth, the wedges were perpendicular to the direction of the incident radiation. For the other materials, 0° azimuth was chosen such that one of the 4 edges of the absorber was perpendicular to the incident radiation. Both HH (horizontal transmit/horizontal receive) and VV (horizontal transmit/vertical receive) radar cross sections were measured. Since the general azimuthal behavior of the absorber's RCS was similar for all elevation angles studied, only the data for the lowest and highest elevation angles are shown in Figures 4-9 for clarity. In addition, the HH and VV RCS behavior as a function of azimuth angle were similar, therefore only the results for horizontal polarization are shown. However, TK THz RAM had a distinctly different RCS behavior at different elevation angles, so all the measured plots of this material are shown in Figure 10.

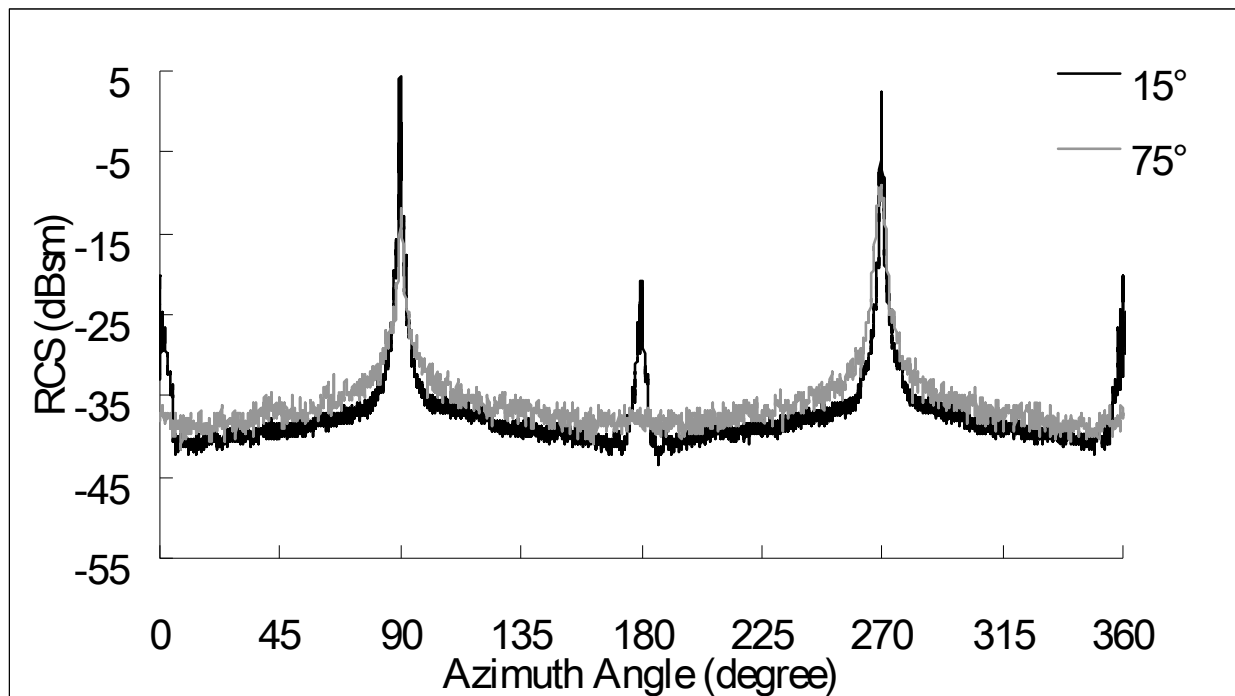


Fig. 4. HH RCS of FIRA™-160 at 15° and 75° elevation.

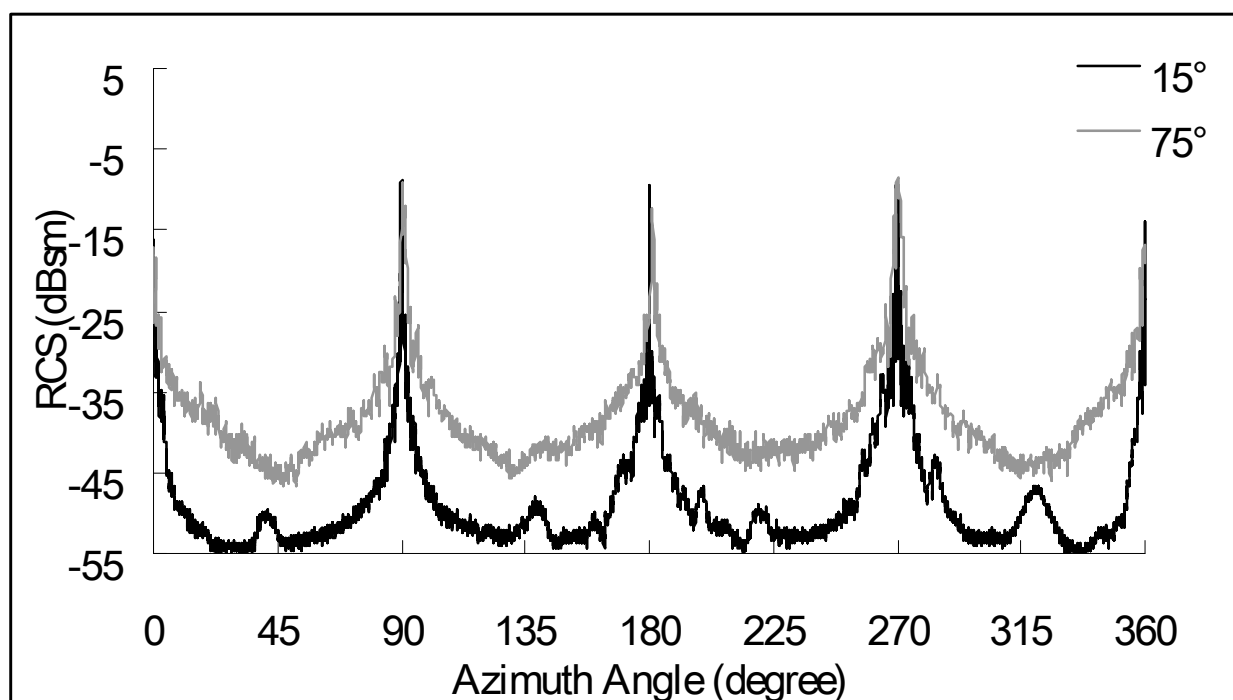


Fig. 5. HH RCS of FIRA™-500-red at 15° and 75° elevation.

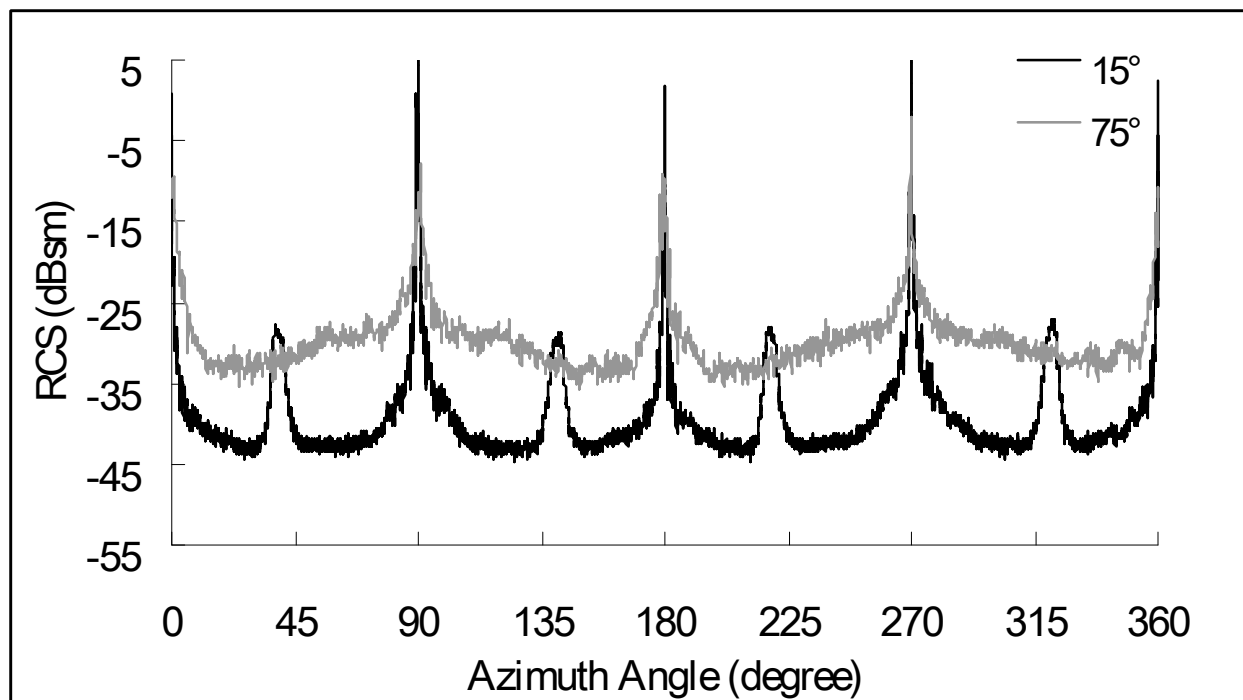


Fig. 6. HH RCS of FIRA™-500-black at 15° and 75° elevation.

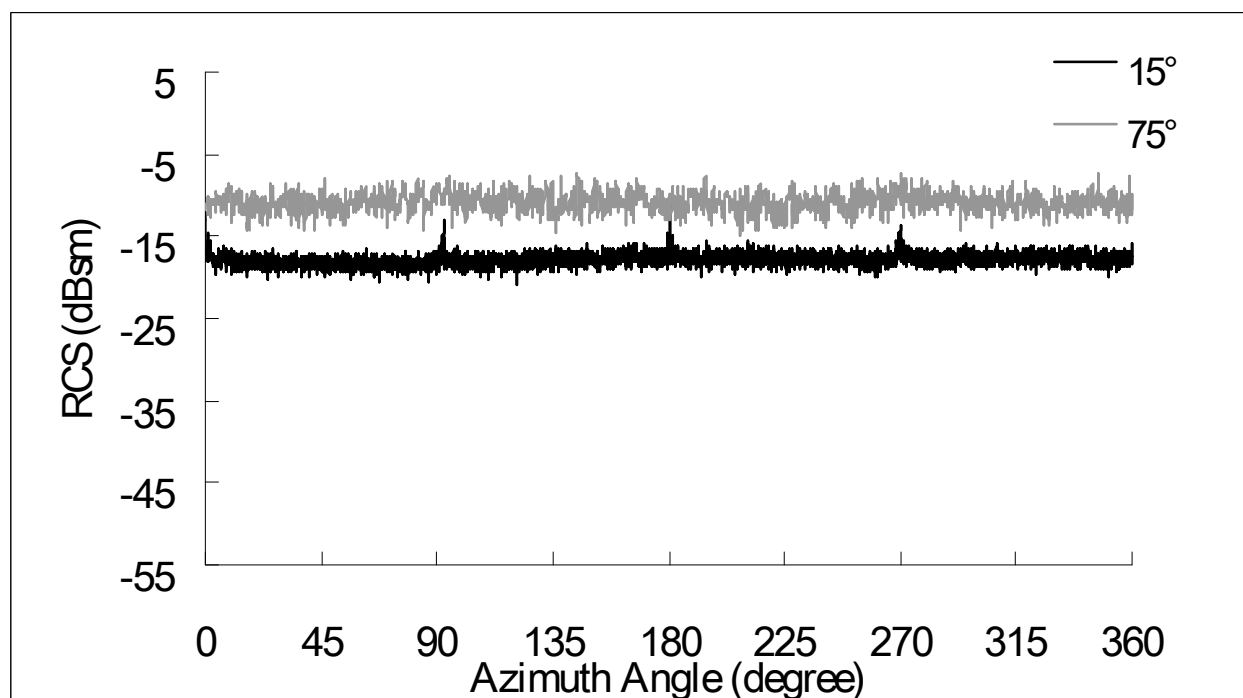


Fig. 7. HH RCS of Rex Mat at 15° and 75° elevation.

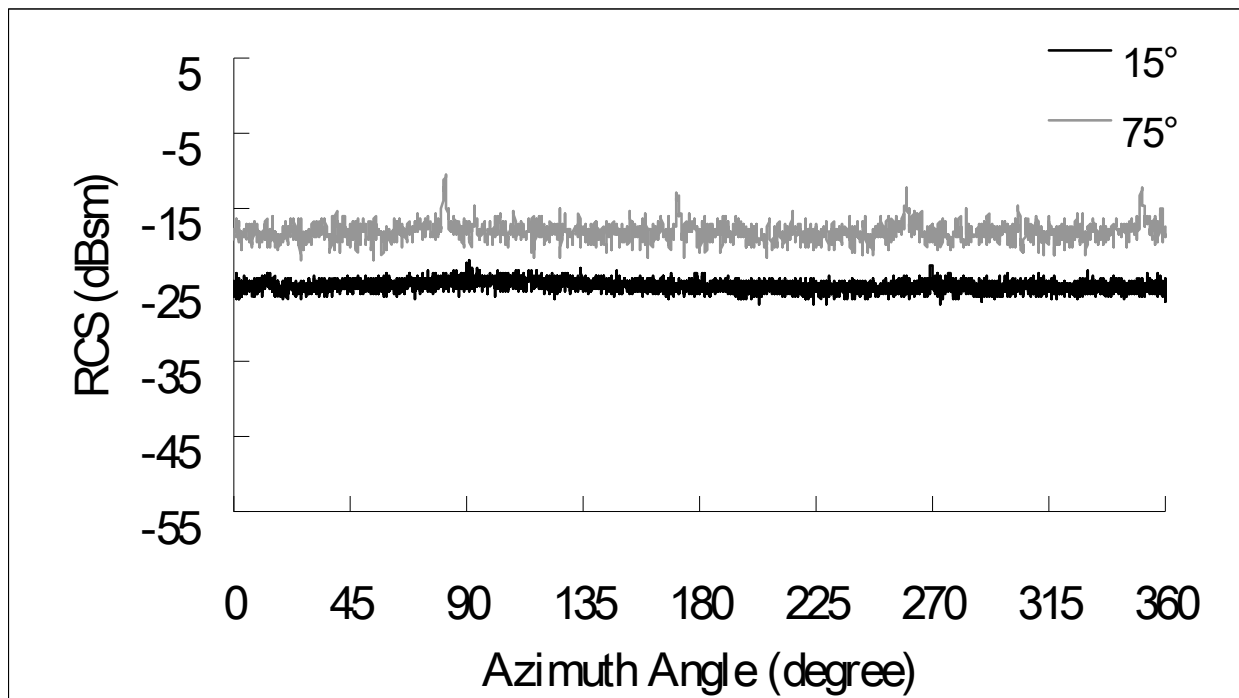


Fig. 8. HH RCS of AEL at 15° and 75° elevation.

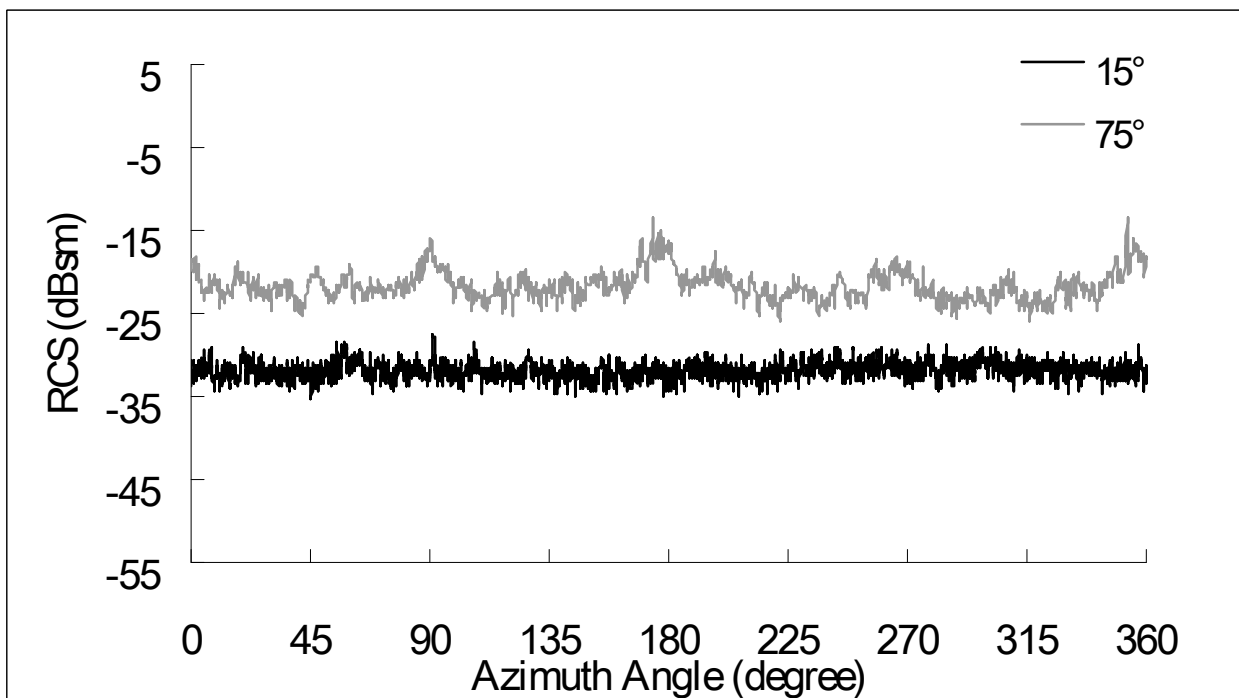


Fig. 9. HH RCS of neoprene wetsuit at 15° and 75° elevation.

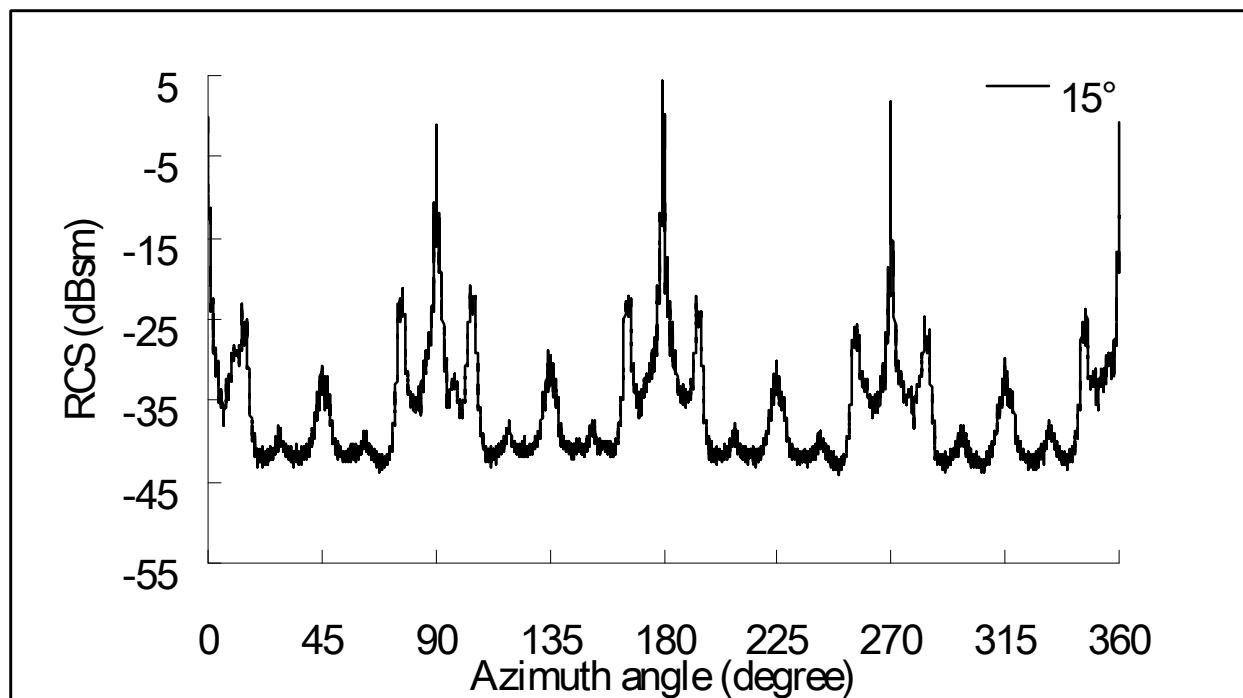


Fig. 10(a). HH RCS of TK THz RAM at 15° elevation.

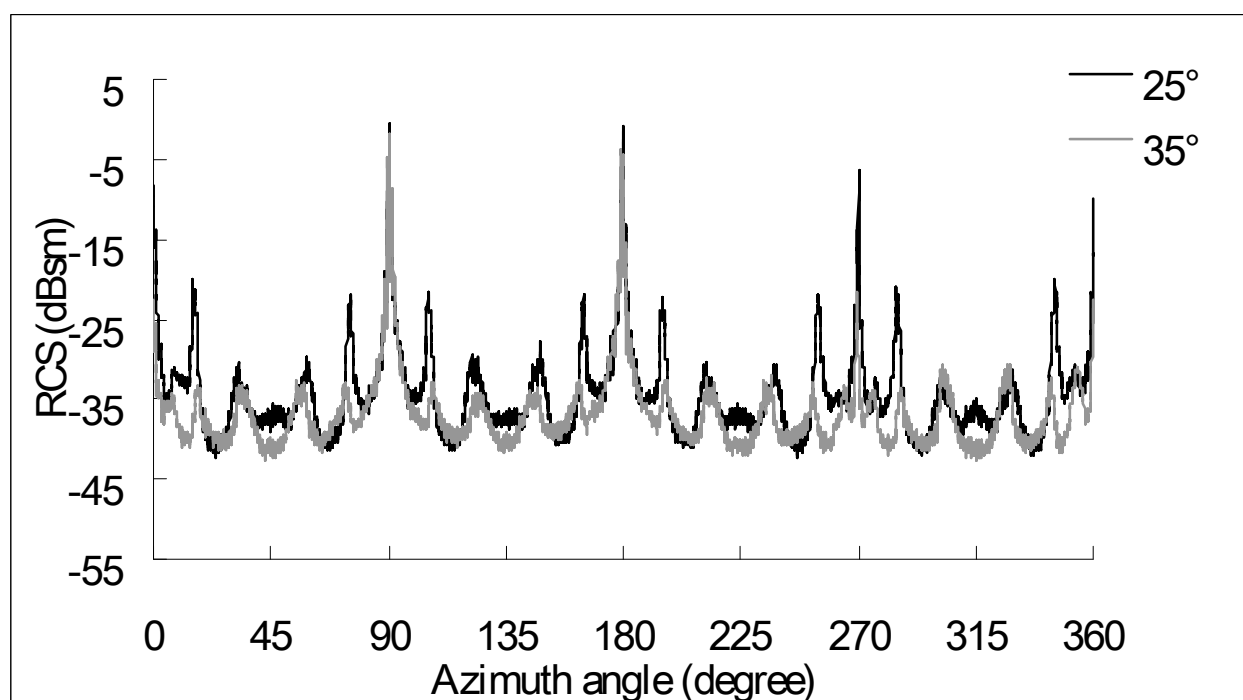


Fig. 10(b). HH RCS of TK THz RAM at 25° and 35° elevation.

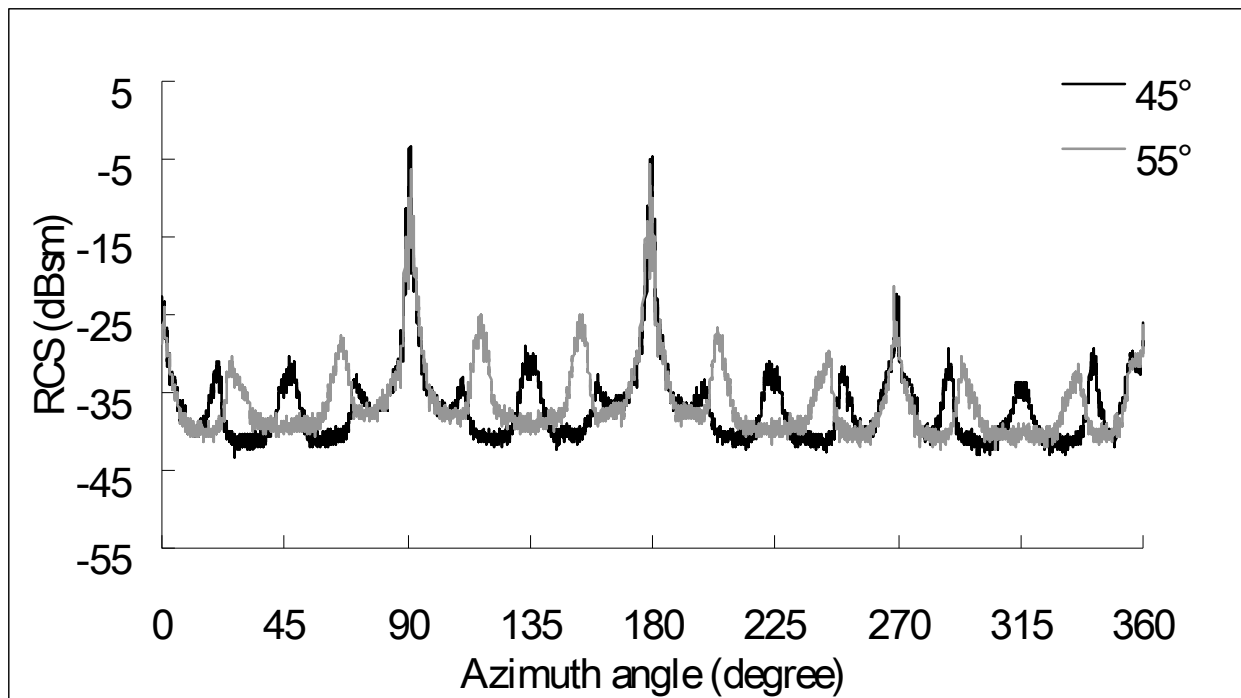


Fig. 10(c). HH RCS of TK THz RAM at 45° and 55° elevation.

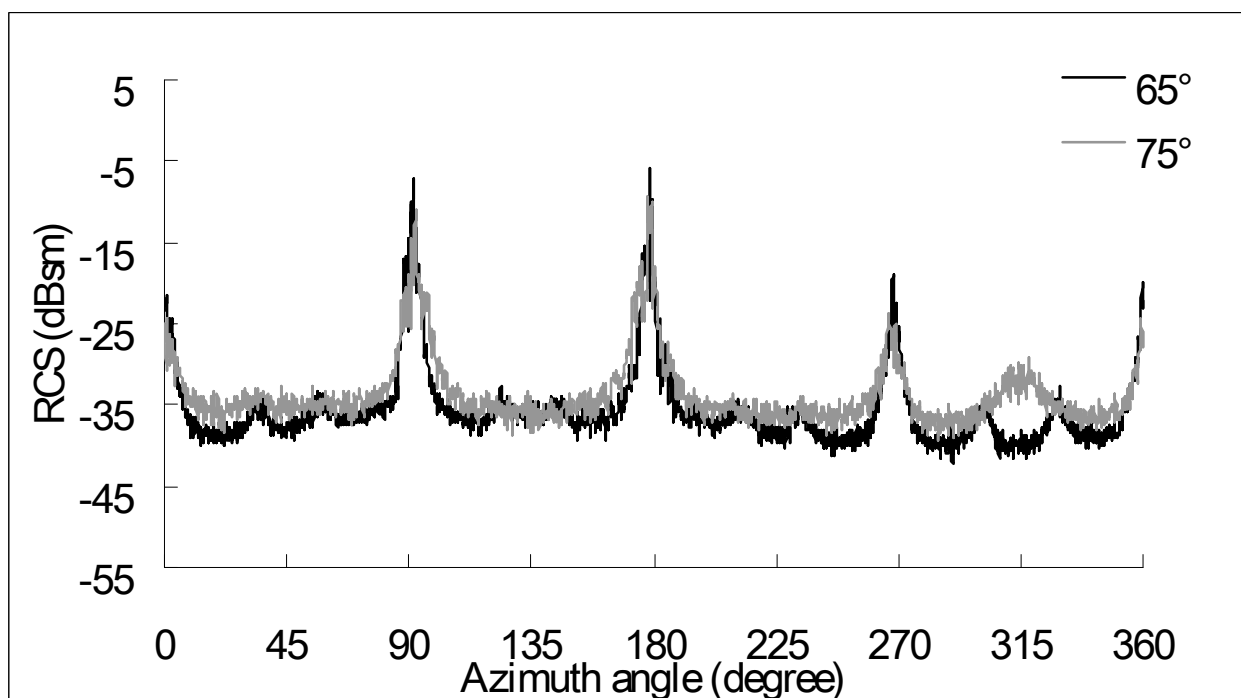


Fig. 10(d). HH RCS of TK THz RAM at 65° and 75° elevation.

The median values of the HH RCS of all materials are shown in Table 1. In each case, the absorber's RCS increased as the elevation angle increased. Since the azimuthal dependence of the absorber's median HH RCS were similar for all elevation angle studied, only the value for the lowest and highest elevation angles are shown.

Table. 1. The median-value of HH RCS at 15° and 75°.

Material	Median-value of RCS (dBsm)	
	15° elevation	75° elevation
FIRAM™-160	-38.8	-34.8
FIRAM™-500-red	-51.2	-39.6
FIRAM™-500-black	-41.4	-30.4
Rex Mat	-17.8	-10.8
AEL	-25.2	-18.0
Neoprene wetsuit (6 layers)	-31.9	-21.9
TK THz RAM	-39.2	-34.9

4.2 Transmittance of materials

The polarized, normal incidence transmittance of the materials was evaluated and shown in Table 2. In Table 2, parallel and perpendicular refer to the direction of the incident electric field relative to the direction of the wedges (or the fabric direction in the case of Rex Mat.)

Table. 2. Transmittance of materials at 160 GHz.

Material	(dB)
FIRAM™-160	-61.0 (parallel), -54.6 (perpendicular)
FIRAM™-500-red	-9.6 (parallel), -9.0 (perpendicular)
FIRAM™-500-black	-48.8 (parallel), -60.5 (perpendicular)
Rex Mat	-12.9 (parallel), -16.0 (perpendicular)
AEL	-23.1
Neoprene wetsuit (6 layers)	-10.7
TK THz RAM	-41.7

4.3 THz imagery of the materials

Data collected in the 160 GHz compact range were processed into two-dimensional inverse synthetic aperture radar (ISAR) imagery. Selected ISAR imagery of FIRAMTM-160 at an elevation angle of 35° is shown in Figure 11. In these images, dark areas represent a higher RCS. Selected ISAR imagery of TK THz RAM at an elevation angle of 35° is shown in Figure 12.

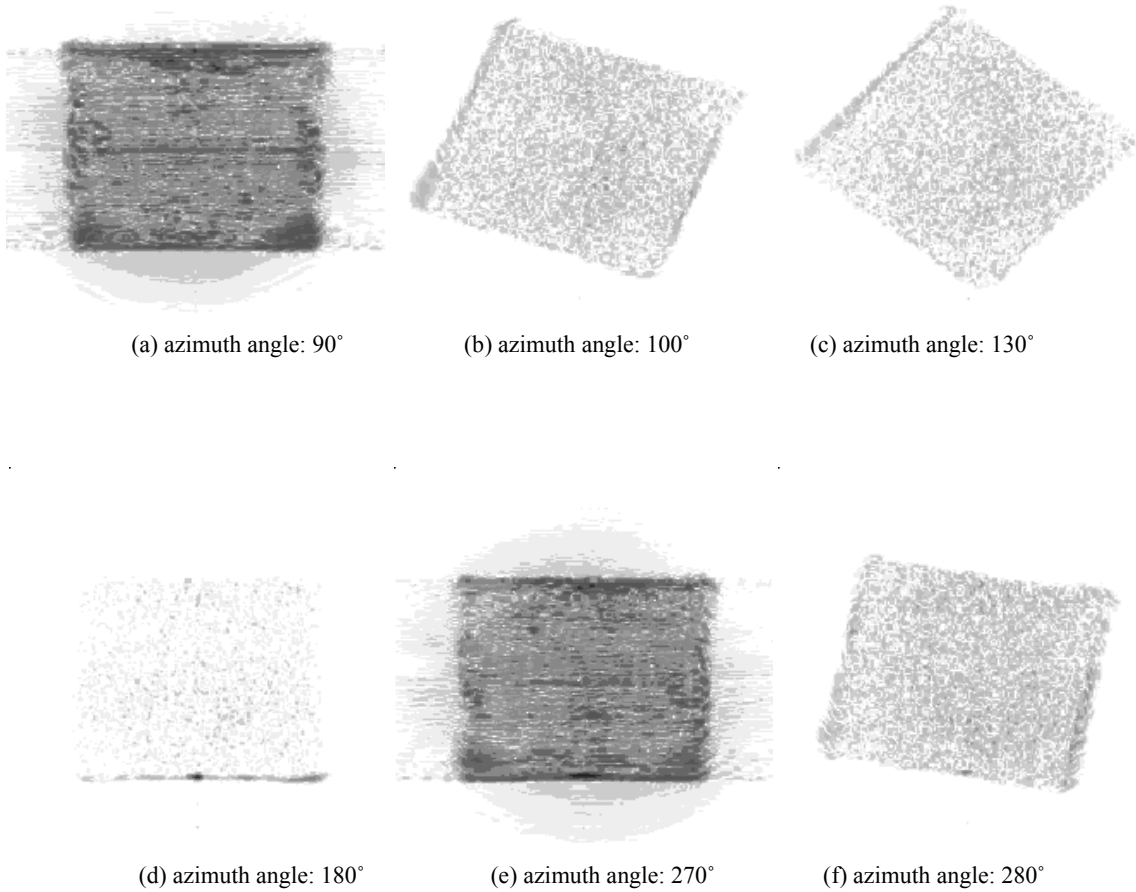


Fig. 11 (a) through (f) ISAR imagery of FIRAMTM-160 at an elevation angle of 35°.

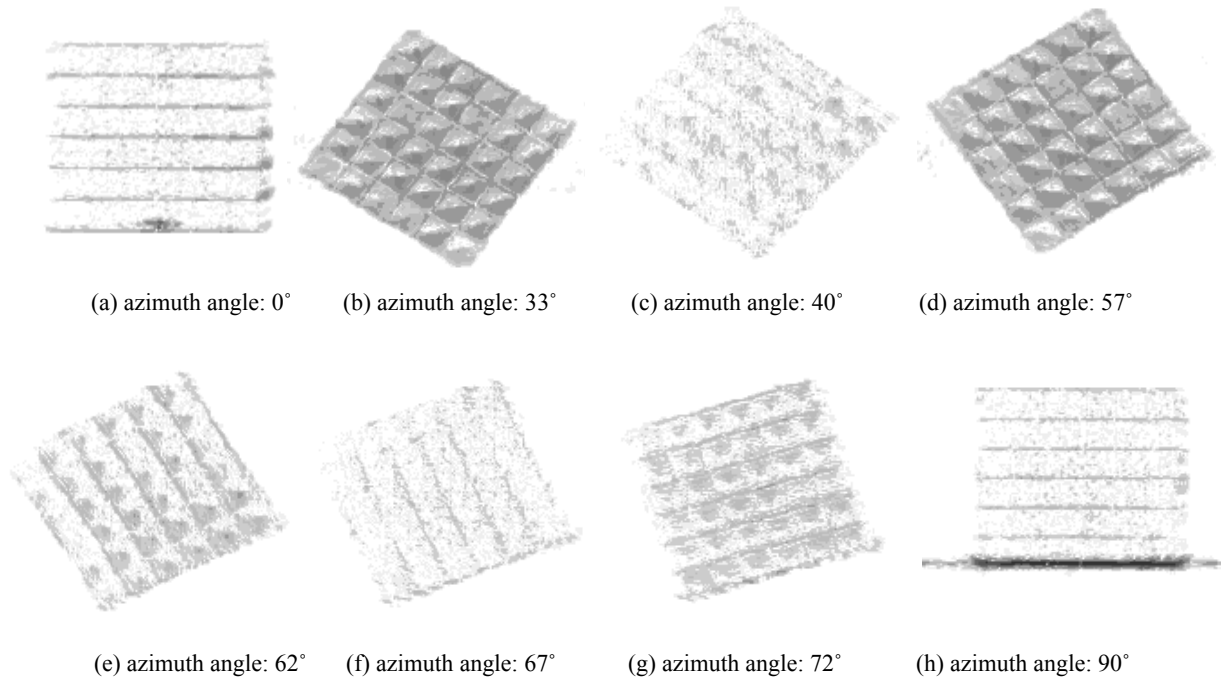


Fig. 12 (a) through (h) ISAR imagery of TK THz RAM at an elevation angle of 35°.

5. DISCUSSION

The backscattering behavior of the wedged absorbers was found to vary significantly with azimuth angle, as expected. When the azimuth angle of these absorbers was such that the wedge direction was oriented perpendicular to incident radiation, a large RCS peak was observed. However, this scattering behavior explains only two of the four RCS peaks observed over the 360-degree azimuth sweep in Figure 4-6. The other peaks observed at 0° and 180° azimuth were found to be a result of backscattering from the 2 ft. long leading and trailing edges of the wedged absorber. Therefore, some portion of the scattering observed at 90° and 270° azimuth was due to edge scattering. Additional scattering peaks were observed in FIRAM™-500-red and FIRAM™-500-black at azimuth angles of 45°, 135°, 225°, and 315°. Analysis of the ISAR imagery demonstrated that these peaks were also due to high levels of backscattering from the material's edges. In a practical setting such as an anechoic radar chamber, individual absorbers would be carefully joined together into large panels and the edge scattering from an individual sheet would be substantially reduced.

FIRAM™-500-red had the lowest medianized RCS of all the absorbers studied. However, the transmittance of FIRAM™-500-red was quite high (-9.6 dB in parallel direction, and -9.0 dB in perpendicular direction). Any radiation that passed through the absorber, specularly reflected off the smooth supporting plate and therefore was not measured by the radar. Because of FIRAM™-500-red's high transmittance, a meaningful RCS comparison between this absorber and others is difficult. The other absorber with a high 160 GHz transmittance was the neoprene wetsuit. Even though 6 layers of this material were used, the transmittance was still quite high (-10.7 dB). In contrast to the FIRAM™-500-red, a relatively high RCS was observed from this material, and was attributed to the scattering caused by the inhomogeneity of this material. Working at a higher frequency would certainly reduce the neoprene wetsuit's transmittance. The fact that it scatters 160 GHz radiation (and therefore higher frequency radiation as well) implies that it would be a rather poor candidate for a high performance THz absorbing material. Higher volumetric scattering was also likely the cause of the relatively high THz RCS observed from the AEL absorber and Rex Mat.

The backscattering behavior of the TK THz RAM and FIRAM™-160 were similar. Sheets of both absorber types had medianized HH RCS values of approximately -40 dBsm to -35 dBsm. FIRAM™-160 and TK THz RAM also had the lowest normal-incidence transmittance. The transmittance of FIRAM™-160 was -61.0 dB in parallel direction and -54.6 dB in perpendicular direction. The transmittance of TK THz RAM was -41.7 dB.

TK THz RAM displayed a particularly interesting RCS behavior. Due to the nature of this pyramidal absorber, several peaks were observed in the RCS vs. azimuth plot (Figure 10). Specifically, the spacing between the RCS peaks was observed to increase with elevation angle. At an elevation angle of 15° the spacing between RCS peaks was about 15° and at elevation angles of 25° and 35° the spacing was about 18°. The spacing at 45° and 55° elevation was 22.5° and 30°, respectively. When the elevation angle became larger, i.e., 65° and 75°, the RCS spacing extended to about 90°.

Each selected material is suitable for its own intended application; however, the measurements presented here were performed over a limited range of angles and at a single frequency (160 GHz). For example, some of the materials are designed for higher elevation angle that wasn't covered in this study. Therefore, measuring these materials at their intended angles and frequency would be the further research.

6. CONCLUSION

The Submillimeter-Wave Technology Laboratory at the University of Massachusetts Lowell has investigated the electromagnetic scattering behavior of various broadband absorbers. The wedged absorbers displayed high RCS when the wedges were oriented perpendicular to incident radiation. In general, the other scattering features observed from the wedged absorbers were found to be due to edge scattering behavior. The RCS of the three "uniform" materials (AEL, neoprene wetsuit, and Rex Mat) were generally independent of azimuth angle and their relatively high RCS was attributed to volumetric scattering. The pyramidal absorber (TK THz RAM) was found to have a number of interesting scattering peaks that were observed periodically in azimuth. However these features diminished as the elevation angle was increased. At 75° elevation, close to where this material is likely designed to be used, these features were substantially reduced.

ACKNOWLEDGEMENT

This work was supported by the National Ground Intelligence Center under US Army contract W911W4-06-C-0020.

REFERENCES

- [1] William H. Emerson, "Electromagnetic wave absorbers and anechoic chambers through years", IEEE, Vol. 21, 484-490, 1973.
- [2] Anne Lönnqvist, Aleksi Tamminen, Juha Mallat, and Antti V. Räisänen, "Monostatic Reflectivity Measurement of Radar Absorbing Materials at 310GHz", IEEE, Vol. 54, 3486-3491, 2006.
- [3] Aleksi Tamminen, Anne Lönnqvist, Juha Mallat, and Antti V. Räisänen, "Monostatic Reflectivity and Transmittance of Radar Absorbing Materials at 650 GHz", IEEE, Vol. 56, 632-637, 2008.
- [4] R. H. Giles, and T. M. Horgan, "Silicone-Based Wedged-Surface Radiation Absorbing Material", U. S. Patent Number 5,260,513, Nov. 1993
- [5] M. Coulombe, T. Horgan and J. Waldman, J. Neilson, S. Carter, and W. Nixon, "A 160 GHZ Polarimetric Compact Range for Scale Model RCS Measurements", Antenna Measurements and Techniques Association (AMTA) Proceedings, Seattle, WA, pg 239, 1996.
- [6] M. Coulombe, J. Waldman, R. Giles, A. Gatesman, T. Goyette, and W. Nixon, "Submillimeter-Wave Polarimetric Compact Ranges for Scale-Model Radar Measurements", Microwave Symposium Digest, 2002 IEEE MTT-S International Vol. 3, 1583-1586, 2002.